GEO-ELECTRIC INVESTIGATION OF GROUNDWATER SYSTEM IN UWASOTA AND ENVIRONS, BENIN CITY, SOUTHERN NIGERIA.

BY

Joseph Ede IDODIA

PSC2003846

TO

DEPARTMENT OF GEOLOGY

FACULTY OF PHYSICAL SCIENCE

UNIVERSITY OF BENIN

BENIN CITY

FEBRUARY, 2025

GEO-ELECTRIC INVESTIGATION OF GROUNDWATER SYSTEM IN UWASOTA AND ENVIRONS, BENIN CITY, SOUTHERN NIGERIA.

BY

Joseph Ede IDODIA

PSC2003846

A PROJECT WORK SUBMITTED TO

THE DEPARTMENT OF GEOLOGY,

FACULTY OF PHYSICAL SCIENCES,

UNIVERSITY OF BENIN,

IN PARTIAL FULFILMENT OF THE REQUIREMENT FOR THE AWARD OF A BACHELOR OF SCIENCE DEGREE (B.Sc) IN GEOLOGY

FEBRUARY, 2025

CERTIFICATION

This is to certify that this project was submitted and approved by the department of Geology in partial fulfilment for the requirement for the award of the Bachelor of Science in Geology, University of Benin, Benin City.

_____ _____

PROJECT SUPERVISOR DATE

(Dr. S. A SALAMI)

_____ _____

HEAD OF DEPARTMENT DATE

(Dr. S. A SALAMI)

DEDICATION

This work is first and foremost dedicated to God, followed by my ever-loving parents my Mom and Dad(late) and siblings who have consistently supported me throughout my life.

ACKNOWLEDGEMENT

This project would not have been possible without my deepest gratitude to God for His guidance and protection over myself, my family and loved ones.

I would like to express my sincere appreciation to my supervisor, Dr. S. A. Salami, who has been a constant source of support and mentorship, not just for me but for all the students in the Geology Department.

I want to express my immense gratitude to the entire staff of the Geology Department, including the wonderful lecturers like Dr. (Mrs) Odokuma Alonge, Dr. O. Alex. Ogbamikhumi, Dr. Nosa. S. Igbinigie, Dr (Mrs) Andre. T. Obayanju and Dr. Maju Oyovwikowhe, and Mr. Muyiwa as well as all the other lecturers and non-academic staffs. Their dedication and support have made my academic journey truly remarkable.

I extend my heartfelt thanks to all my friends and classmates who have helped me in various ways, as well as to my dedicated group members who collaborated with me on this project.

Finally I am also incredibly grateful to my loving parents, Mr. Maxwell U. IDODIA (Late), Mrs. Blessing IDODIA, and my siblings for their unwavering support, especially during challenging times.

TABLE OF CONTENTS

TITLE PAGE

CERTIFICATION

DEDICATION

ACKNOWLEDGEMENT

TABLE OF CONTENTS

LIST OF FIGURES

LIST OF TABLES

LIST OF PLATES

ABSTRACT

CHAPTER ONE

INTRODUCTION

1.1 GENERAL STATEMENT

1.2 AIM AND OBJECTIVES

1.3 LOCATION OF STUDY AREA

1.4 COMMON METHODS OF GEOPHYSICAL INVESTIGATION

1.5 ELECTRODE ARRAY

1.6. SCHLUMBERGER ARRAY:

1.7. WENNER ARRAY

1.8 Advantages of the Schlumberger array over the Wenner array

1.9 Advantages of the Wenner array over the Schlumberger array

CHAPTER TWO

LITERATURE REVIEW AND GEOLOGIC SETTING

2.1 GENERAL GEOLOGY

2.2 REGIONAL GEOLOGY

2.2.1 TECTONIC SETTING

2.2.2 STRATIGRAPHIC SETTING

2.2.3 MODERN DELTA STRATIGRAPHY

CHAPTER THREE

MATERIALS AND METHODS

3.1 LIST OF EQUIPMENT

3.2 THEORY OF RESISTIVITY

3.3 FIELD PROCEDURE

3.4 DATA ACQUISITION

3.5 FIELD PRECAUTIONS

3.6 ADJUSTED DATA

3.7 INTERPRETATION TECHNIQUE

CHAPTER FOUR

RESULTS AND DISCUSSION

4.1 RESULTS

4.2 DISCUSSION

CHAPTER FIVE

CONCLUSION

5.1 CONCLUSION AND SUGGESTION FOR FURTHER STUDIES

5.2 SUGGESTION FOR FURTHER STUDIES

REFERENCES

LIST OF FIGURES

Figure 1.1: Topograpic Map of the Study Area

Figure 1.2: Electrode array

Figure 1.3 : Schlumberger Array.

Figure 1.4: Diagrammatic representation of Wenner

Figure 2.1: Major Litho-Petrological Units in Nigeria.

Figure 2.2: Stratigraphy of the Niger-Delta.

Figure 3.1: Equipotential and current lines for a pair of current electrodes A and B on a homogeneous half-space.

Figure 3.2: Resistivity curves (after Gopinath & Seralathan, 2003).

Figure 4.1: VES1 interpretation results.

Figure 4.2: VES2 interpretation results.

Figure 4.3: VES3 interpretation results.

Figure 4.4: VES4 interpretation results.

Figure 4.5: Map of Surface Elevation

Figure 4.6:Map of depth to Depth to water table

Figure 4.7: Equi-potential map

Figure 4.8: Map of Iso-resistivity

Figure 4.9: Local Groundwater flow

LIST OF TABLES

Table 1: Results for VES JJV1

Table 2: Results for VES JJV2

Table 3: Results for VES JJV3

Table 4: Results for VES JJV4

Table 5: Geological model of VES JJV1

Table 6: Geological model of VES JJV2

Table 7: Geological model of VES JJV3

Table 8: Geological model of VES JJV4

Table 9: Hydrogeological representation of the VES Data

LIST OF PLATES

Plate 1: The Tetrameter (ABEM Tetrameter 300)

Plate 2: Cable reels

Plate 3: Connecting Cables.

Plate 4: Hammer

Plate 5: Electrodes

Plate 6: Measuring tapes.

Plate 7: Picture of a GPS

Plate 8: Battery (backup)

ABSTRACT

Groundwater potential assessment using the Vertical Electrical Sounding (VES) technique was conducted in Uwasota and environs, Benin City, Southern Nigeria. Four VES measurements were acquired using the Schlumberger electrode array. The data were quantitatively interpreted using curve matching and computer iteration techniques to generate geoelectric parameters. The VES results revealed subsurface lithologies consisting of topsoil, lateritic soil, dry sand, and saturated sand, all within the Benin Formation. Resistivity analysis allowed for the delineation of potential aquifer zones and estimations of groundwater depth. This study provides valuable insight into the subsurface hydrogeological conditions and delineates areas suitable for groundwater development in Uwasota and environs, contributing to improved groundwater resource management in the region.

CHAPTER 1

INTRODUCTION

GENERAL STATEMENT

The challenge of securing a sufficient supply of quality water is increasingly problematic due to the rise in population and industrialization. Regarding quality, surface water is not a reliable source throughout the year, thus highlighting the necessity of exploring other alternatives to supplement surface water (Alisiobi and Ako, 2012). Alabi et al. (2010) state that approximately 53% of the population depends on groundwater as a drinking water source. Groundwater refers to the water present beneath the ground surface within soil pores and fractures of geologic formations. To tap into the potential availability of water, geophysical field measurements are conducted to assess the groundwater resources in the study area and to identify optimal locations for borehole drilling (Helaly, 2017). Most underground water originates from precipitation that has infiltrated into the earth. Observations indicate that a significant portion of excess rainfall runs off the ground surface, while another portion infiltrates underground, becoming groundwater that feeds springs, lakes, and wells (Oseji et al., 2006). A rock unit or unconsolidated deposit is termed an aquifer if it can yield a usable quantity of water (Alabi et al., 2010). Geoelectrical methods are especially suitable for groundwater research because hydrogeological properties, such as porosity and permeability, can be linked to electrical resistivity values. Geoelectrical techniques focus on measuring the electrical resistivities of subsurface materials, which provides preferential insights into various geological layers, structures, and the corresponding presence of groundwater (Stewart 1982; Danielsen et al., 2007; Nowroozi et al., 1999; Meju, 2005). The Vertical Electrical Sounding (VES) technique offers information on the vertical changes in ground resistivity with depth, while the Constant Separation Traversing (CST) method allows for determining interval changes in ground resistivity (USEPA, 2000; Ariyo, 2005; OEPA, 2008). The application of geophysical methods for both mapping groundwater resources and evaluating water quality has significantly increased in recent decades due to rapid advancements in electronic technology and the evolution of numerical modeling solutions (Olayinka, 1992; Metwaly et al., 2009; Ndlovu et al., 2010). Although various hydrogeophysical techniques are available, electrical resistivity remains a favored method because of its affordability, straightforward operation, and effectiveness in

regions with contrasting resistivity, such as between weathered overburden and bedrock (Telford et al., 1990). Geophysical investigations of the earth entail taking measurements at or near the earth's surface that are impacted by the internal distribution of physical properties. Geophysics is also regarded as the subsurface characterization of geology, geological structures, groundwater, contamination, and human artifacts beneath the Earth's surface, based on the lateral and verticalmapping of physical property variations that are remotely assessed using non-invasive technologies (Afuwai, 2013).

1.2 AIM AND OBJECTIVES

This research work aims at investigating the groundwater potential of the study area by the using vertical electrical sounding (VES) technique.

The following are the objectives

1. Delineation of the subsurface lithology using resistivity values.
2. Identifying the groundwater prospect of the study area

1.3 LOCATION OF STUDY AREA

1.4 COMMON METHODS OF GEOPHYSICAL INVESTIGATION

Gravity Method: The gravity method consists of measuring fluctuations in the Earth's gravity field that arise from variations in the density of underground rocks. This technique is often linked to extensive regional geophysical surveys aimed at examining geological structures at substantial depths. Gravity measurements can also be conducted from airborne platforms or in marine environments. In earlier ground investigations, gravity data were primarily utilized to create contour maps that identified anomalous areas related to density decreases in surface materials, which could indicate the presence of voids or abandoned mine shafts, for instance. For specific applications, like detecting near-surface cavities, the gradient of the Earth's gravity field can be assessed. In larger engineering surveys, this method has helped identify sizable fault lines, deeply buried channels, and rock formations in back-filled quarries.

Magnetic Method: The magnetic method utilizes a magnetometer to passively assess the Earth's magnetic field at various points on the surface. Magnetic data anomalies can suggest the existence of subsurface areas with high magnetic susceptibility, aiding in site characterization (Burger et al., 2006; Telford et al., 1990).

Electrical Methods: The electrical method encompasses various approaches, which can be classified as either passive, relying on the Earth's natural electric field, or active, using artificial currents. These methods employ direct currents or low frequency alternating currents to explore the electrical characteristics of the subsurface (Kearey et al., 2002).

Seismic Methods: This method employs sound or acoustic waves known as seismic waves. While seismic waves are typically produced during earthquakes, those used in geophysical surveys are artificially generated, categorizing this as an active method; however, passive seismic geophysics also exists for earthquake studies and understanding Earth's structure. In seismic surveys, waves are created by a controlled source and travel through the subsurface, with some waves reflecting or refracting off geological boundaries and returning to the surface. Instruments placed along the surface to measure the resulting ground motion from these returning waves, allowing for the calculation of arrival times at varying distances from the source. These travel times can be converted into depth measurements, enabling systematic mapping of subsurface geological interfaces (Kearey et al., 2002). Common applications of seismic methods include oil and gas exploration as well as groundwater assessment.

1.5 Electrode Array

An electrode array refers to a setup of electrodes utilized for detecting either electric current or voltage. Some electrode arrays are capable of functioning bidirectional, meaning they can also deliver a stimulating pattern of electric current or voltage. (See Fig. 1.2)

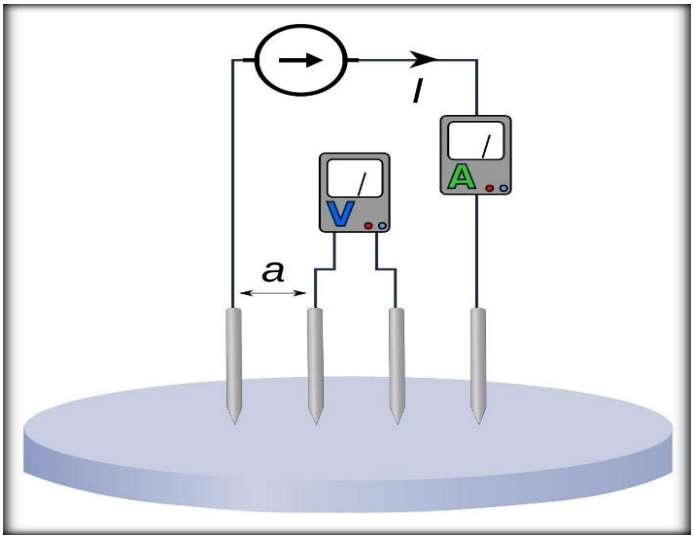

Fig. 1.2: Electrode array

1.6 Schlumberger Configuration

The electrode setup applied in this study is the Schlumberger configuration. The selection of the Schlumberger array is based on its superior resolution and lower labor costs compared to other configurations, such as the Wenner array, Lee partitioning method, pole-dipole method, and others.

This technique employs four aligned electrodes, with the two outer ones serving as current electrodes (C1 and C2) and the two inner ones (P1 and P2) functioning as potential electrodes (Fig. 2.6c). The current electrodes, C1 and C2, are positioned symmetrically around the center O, each at a distance of 1 cm from the center. The inner potential electrodes, on the other hand, are spaced more closely together, being equidistant from O at a separation of 0.2 cm each.

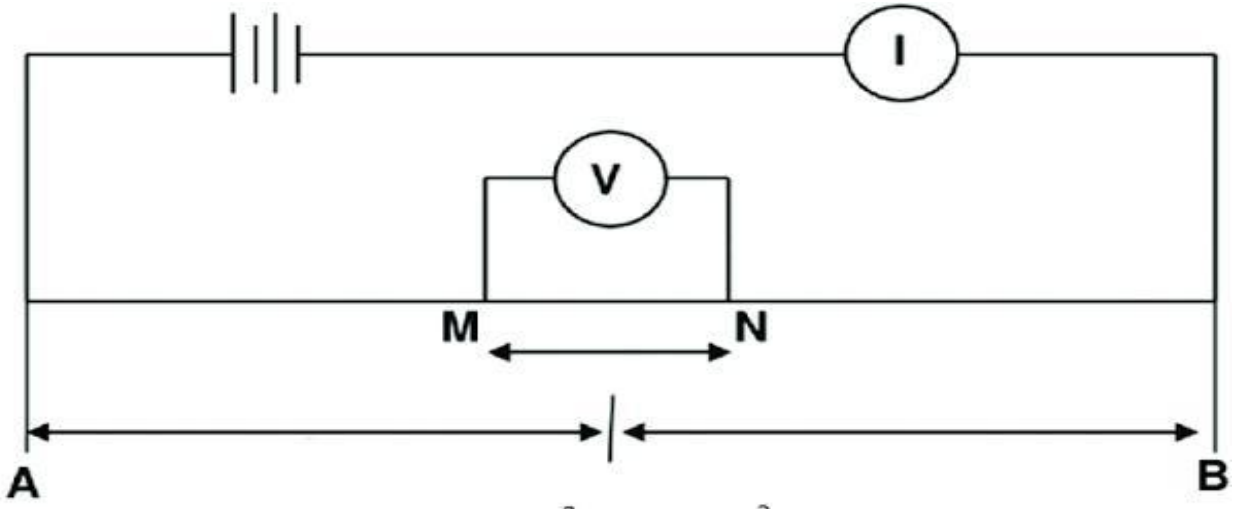

$$P=\pi \frac{(AB/2)^2-(MN/2)^2}{MN}\frac{\Delta V}{I}$$

AB/2 = half current electrode spacing.

MN/2 = half potential electrodes spacing.

ΔV = potential difference measured between the potential electrodes M and N,

I = electric current injected into the ground by the current electrodes A and B.

Fig 1.3: Schlumberger Array

1.7 Wenner Array

The Wenner electrode array is made up of a series of four electrodes placed at equal intervals. Electric current is introduced through the outer electrodes, while the voltage is recorded between the inner electrodes.

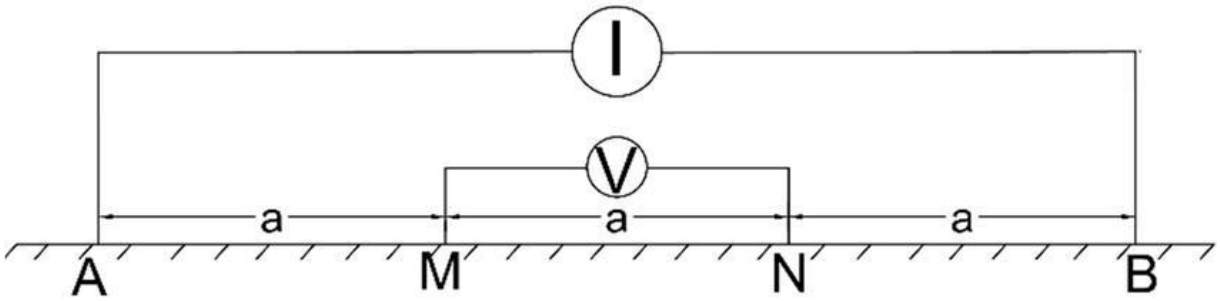

Fig 1.4: Wenner Array

Other Common types of arrays are:

Schlumberger (Wenner)

Wenner alpha

Wenner beta

Wenner gamma

Pole-pole

Dipole-dipole

Pole-dipole

Equatorial dipole-dipole

1.8 Advantages of the Schlumberger array over the Wenner array

The Schlumberger array has the benefit of needing fewer electrode relocations for each measurement, and the distance between the potential electrodes is shorter. Additionally, Schlumberger soundings generally provide better resolution, a deeper level of investigation, and a more streamlined field setup compared to the Wenner array.

1.9 Advantages of the Wenner array over the Schlumberger array

1. A key advantage of the Wenner array is that the apparent resistivity can be readily calculated in the field, and the instrument's sensitivity is less critical compared to other array configurations.

2. Smaller currents are adequate to produce noticeable potential differences.

CHAPTER TWO

LITERATURE REVIEW

2.1 GENERAL GEOLOGY

Nigeria's geology is made up of three main litho-petrological components, which include the Basement complex, Sedimentary Basins, and the Younger Granites (Obaje, 2009). Sedimentary basins are regions of the Earth's crust that are mainly distinguished by subsidence (Watts, 2024). These basins form as negative geological features due to tectonic activities and act as containers for the deposition and accumulation of sediments. The Sedimentary Basins in Nigeria, depicted in Figure 2.1, hold sediments that date from the Cretaceous to Tertiary periods and include the following basins:

Anambra Basin,

Niger Delta Basin,

Dahomey Basin,

Borno Basin,

Bida Basin, Sokoto Basin,

And Benue Trough.

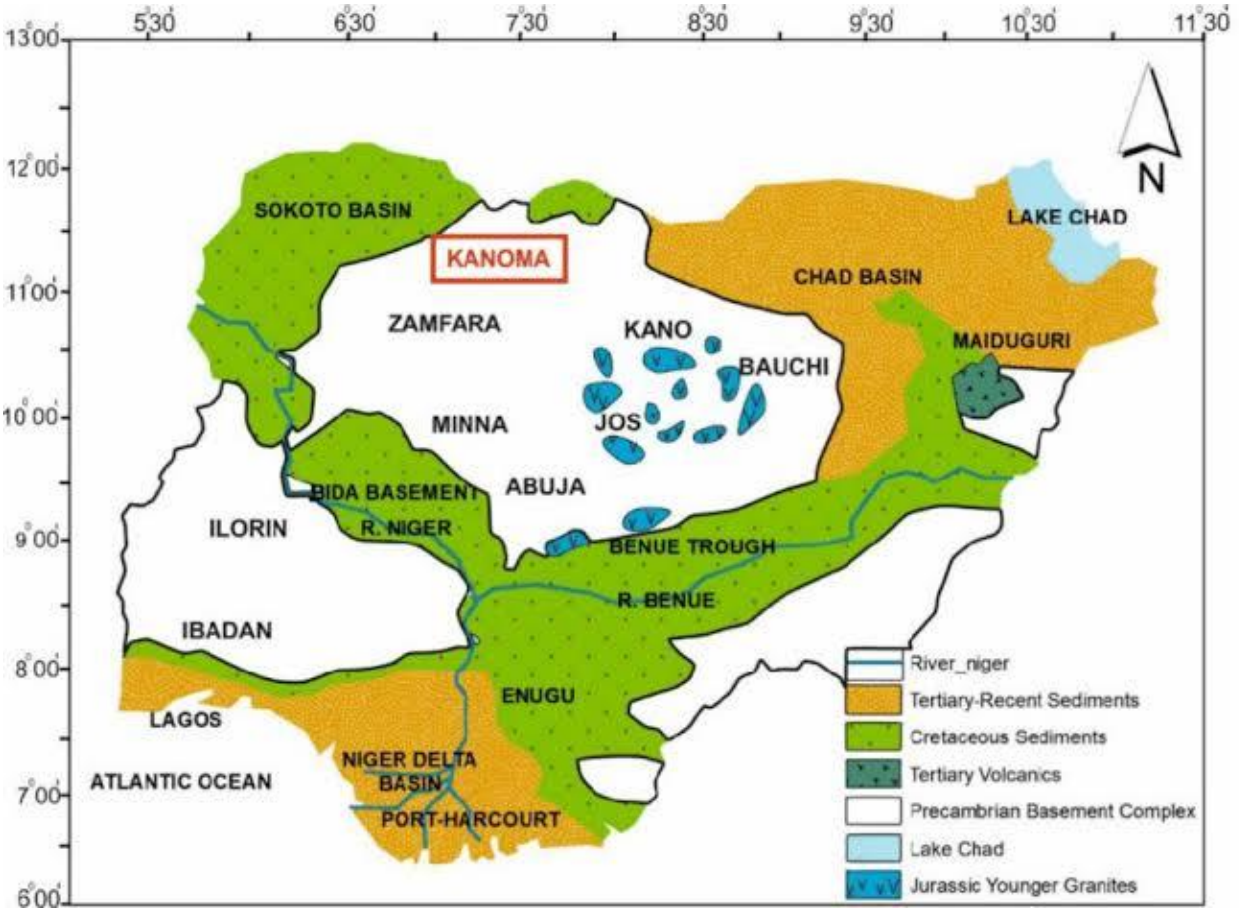

Fig 2.1: Major petrographic regions in Nigeria.

2.2 The Stratigraphy of the Niger Delta The sedimentary layers within the Niger Delta basin are divided into three primary lithofacies units: the Marine shale (Akata Formation), the Marginal marine sandstones, shale, and clays (Agbada Formation), and the extensive continental sandstones (Benin Formation). These formations illustrate an upward-coarsening clastic wedge and were mainly created in marine, deltaic, and fluvial settings. Below is a review of these three geological formations located in the Niger Delta:

2.2.1 BENIN FORMATION

The Benin Formation is situated above the Agbada Formation. The upper part of the Niger Delta elastic wedge consists of coastal plain sands that are present in the Benin-Onitsha area to the north, extending beyond the existing coastline. The upper limit of this formation is characterized by the youngest underlying marine shales and reaches a depth of roughly 1400 meters. The estimated age of the formation is believed to range from the Oligocene to the Recent period. The upper layers of the formation consist of non-marine sands deposited in alluvial or upper coastal plain environments during delta progradation. As it extends further into the basin, the formation gradually thins, eventually diminishing near the shelf edge. The primary deposits are characterized by large, highly porous sandstones capable of storing fresh water, interspersed with some isolated clay layers and limited shale intercalation near the base of the formation. These sands typically exhibit a fine-grained texture and are often granular in nature. The grains tend to be sub-rounded to well-rounded and generally display poor sorting. Owing to a limonitic layer, the sands exhibit a white or yellowish-brown coloration. In some regions, noticeable remnants of plant material and streaks of lignite can be seen, in addition to occurrences of hematite and feldspar grains. Its estimated age ranges from the Miocene to the Recent, though the lack of faunal remains makes precise dating challenging. The thickness of the formation varies from 0 to 2,100 meters, reaching its maximum in the central delta area, where subsidence is most pronounced. The Benin Formation exhibits features attributed to partly marine, deltaic, estuarine, and lagoonal environments, indicating its formation in a continental upper deltaic setting.

2.2.2 AGBADA FORMATION

The Agbada Formation is identified as a paralic sequence, characterized by interbedded shales and sands distributed throughout the Niger Delta's clastic wedge. With increasing depth, the thickness of the shale layers grows while the sand layers become thinner. This formation achieves a maximum thickness of around 3,900 meters and is dated from the Eocene to the Pleistocene. Located in southern Nigeria, it is known locally as the Ogwashi-Asaba and Ameki Formations. The lithological makeup consists mainly of alternating sands, silts, and shales, showcasing gradual variations in grain size and bed thickness. These layers are typically understood to have developed in fluvial-deltaic settings. Beneath the Benin Formation, the Agbada Formation is made up of interlayered fluvio-marine sands, sandstones, and siltstones in various proportions and thicknesses,

showcasing a cyclical arrangement of offlap units. The sandstone exhibits a variety of textures, ranging from coarse to fine grain, with degrees of sorting from poorly sorted to very well sorted, and varying from unconsolidated to slightly consolidated. Some shell fragments and glauconites display signs of a limonite streak and coating. The shales are medium to dark grey in color, well-consolidated, and silty, containing dispersed glauconites. There is a gradual transition into the Akata Formation as the shale content becomes more pronounced. The Agbada Formation consists of a complex mix of deposits formed in at least five different environments: holomarine, barrier bar, barrier foot, tidal coastal plain, and lower deltaic flood plain. Its thickness ranges from 0 to 4500 meters.

2.2.3 AKATA FORMATION

Located in the central region of this clastic wedge is the Akata Formation, predominantly composed of prodeltaic dark grey shales and silts, with sporadic sand streaks that may result from turbidite flows, reaching an estimated thickness of 6,400 meters. Presence of planktonic foraminifera suggests a Paleocene to Recent depositional environment on a shallow marine shelf. The shales located in the northeastern part of the Delta basin, which can be seen onshore, are designated as Imo shale. This formation is also present offshore within diaper structures along continental slopes, where it is considerably buried; Akata shales frequently undergo overpressure. Prodelta and deeper water deposits transition upward into the Agbada Formation, as inferred from the Akata shales. It is believed to be the source rock for the Niger Delta complex.

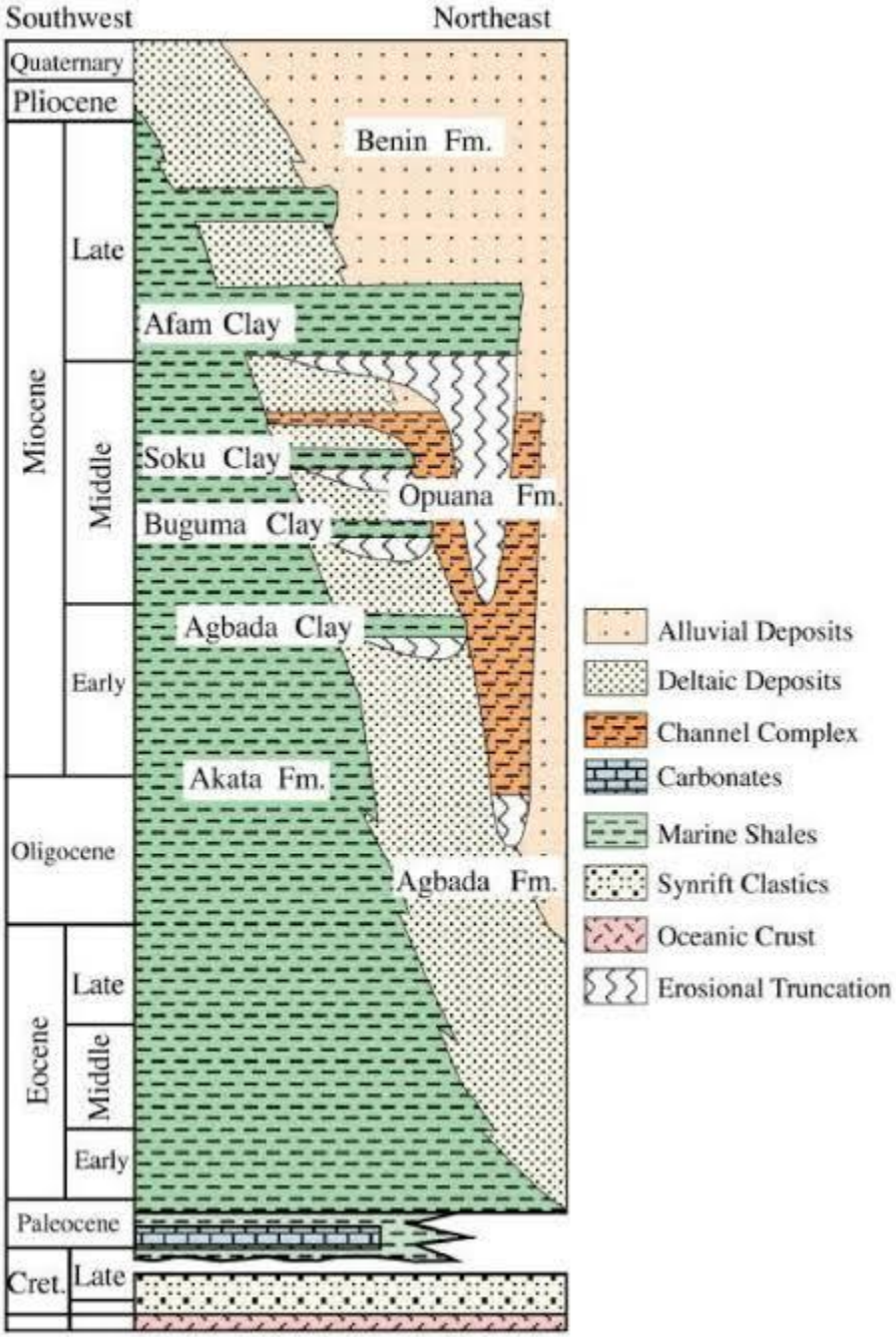

Fig 2.2. Stratigraphic representation of the Niger Delta Basin (Chiaghanam et al., 2018).

CHAPTER THREE

MATERIALS AND METHOD

Tthe equipment used during the fieldwork, comprises:

1. ABEM digital Tetrameter: This instrument (see Plate 1) serves as a signal averaging system referred to as SAS300. It operates in multiple modes and executes four cycles. In its resistivity mode, it features a battery-powered deep-penetrating resistivity meter capable of functioning with current electrode separations of up to 2 km under optimal surveying conditions. The ratio of the generated potential (V) to the supplied current (I) is automatically calculated and averaged over the selected number of cycles, with the outcome displayed digitally in milliohms, ohms, or kilo ohms. The overall measuring range extends from 0.5 milliohm to 1999 kilo ohms. The SAS300 consists of a compact three-unit measurement system, all housed within a single unit. These three components include the transmitter, the receiver, and the microprocessor, which work together as an integrated system to produce the displayed readings. The voltage signal from the transmitted current is captured by the receiver after removing noise from the signal. The microprocessor manages and regulates all measurements to ensure optimal accuracy, performing a thorough one-second check on the circuit and switch position

.Plate 1: The Tetrameter (ABEM Tetrameter 300)

Cable reels: These instruments are used to connect the electrodes to the terrameter

which gives reading,

Plate 2: Cable reels Connecting cables:

They are used to connect the terrameter to the cable reels,

Plate 3: Connecting Cables.

Hammer: The instrument was used to nail electrodes into the ground,

Plate 4: Hammer

Electrodes: The instrument is used to collect data and also marking points,

Plate 5: Electrodes

Measuring tapes: The instrument is used to measure distance in the field,

Plate 6: Measuring tapes.

GPS: The instrument is used to get GPS coordinates and take the elevation of the area where readings were taken from,

Plate 7: Picture of a GPS

Battery (backup): This is used to power the Tetrameter instrument in the field, as a

backup system.

Plate 8: Battery

3.2. THEORY OF RESISTIVITY

Data obtained from resistivity surveys are typically expressed and analyzed in terms of apparent resistivity values, denoted as ρa. Apparent resistivity is characterized as the resistivity of a uniformly homogeneous and isotropic half-space that would produce the observed relationship between the applied current and the resulting potential difference for a specific configuration and spacing of electrodes. By investigating the potential distribution generated by a single current electrode, one can derive an equation that relates apparent resistivity to the applied current, potential distribution, and electrode arrangement. The influence of an electrode pair, or any other configuration, can be determined through the principle of superposition. For instance, consider a solitary point electrode positioned at the boundary of a semi-infinite, electrically homogeneous medium, which serves as a model for a fictitious homogeneous earth. When this electrode conducts a current I, measured in amperes (A), the potential at any location within the medium or along the boundary can be expressed as follows:

$$U = \rho \frac{I}{2\pi r},$$

Equation 1

Where

U = potential, in V,

P = resistivity of the medium,

R = distance from the electrode.

For an electrode pair with current I at electrode A, and -I at electrode B (figure 1), the potential at a point is given by the algebraic sum of the individual contributions:

Equation 2

$$U = \frac{\rho I}{2\pi r_A} - \frac{\rho I}{2\pi r_B} = \frac{\rho I}{2\pi}\left[\frac{1}{r_A} - \frac{1}{r_B}\right],$$

where

rA and rB = distances from the point to electrodes A and B

Figure 1 illustrates the electric field around the two electrodes in terms of equipotentials and current lines. The equipotentials represent imagery shells, or bowls, surrounding the current electrodes, and on any one of which the electrical potential is everywhere equal. The current lines represent a sampling of the infinitely many paths followed by the current, paths that are defined by the condition that they must be everywhere normal to the equipotential surfaces.

Equi-potentials and current lines for a pair of current electrodes A and B on a homogeneous half-space.

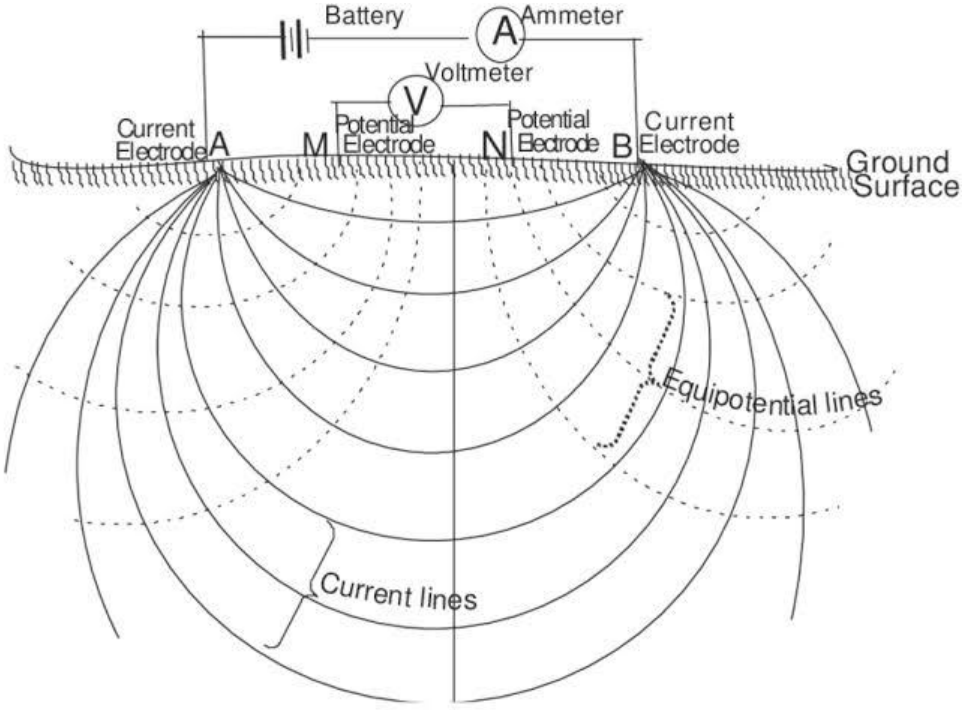

Figure 3.1. Equipotential and current lines for a pair of current electrodes A and B on a homogeneous half-space.

In addition to current electrodes A and B, figure 1 shows a pair of electrodes M and N, which carry no current, but between which the potential difference V may be measured. Following the previous equation, the potential difference V may be written

Equation 3

$$V = U_M - U_N = \frac{\rho I}{2\pi}\left[\frac{1}{AM} - \frac{1}{BM} + \frac{1}{BN} - \frac{1}{AN}\right],$$

Where

UM and UN = potentials at M and N,

AM = distance between electrodes A and M, etc.

These distances are always the actual distances between the respective electrodes, whether or not they lie on a line. The quantity inside the brackets is a function only of the various electrode spacings. The quantity is denoted 1/K, which allows rewriting the equation as:

$$V = \frac{\rho I}{2\pi}\frac{1}{K},$$

Equation 4

Where

K = array geometric factor.

Equation 58 can be solved for ρ to obtain:

Equation 5

$$\rho = 2\pi K \frac{V}{I},$$

The resistivity of the medium can be found from measured values of V, I, and K, the geometric factor. K is a function only of the geometry of the electrode arrangement.

Electrical circuit for resistivity determination an electrical field for a homogeneous datum (after Telford, 1976).

3.3. FIELD PROCEDURE

The fieldwork involved conducting VES traverses at selected locations within the study area. Each VES traverse began by establishing a central point, where an electrode was inserted to act as a reference for measuring the array's spread. The configuration of electrodes used was the Schlumberger array, which required positioning the potential and current electrodes equidistantly around the central point. These electrodes were connected to their respective reels and driven into the ground. Subsequently, the reels were linked to a Tetrameter, which was turned on to take resistance measurements by pressing a button. After each measurement was recorded, the current electrodes were systematically moved further away from the center, followed by taking another reading. This procedure was repeated until the resistance value became too low for measurement, at which point the potential electrodes were also spaced out further, and the current intensity was increased to obtain stronger readings. This process continued until the predetermined spread limit was attained. The accurate placement of electrodes from the

center was directed by the point-per-decade protocol, with this study employing the 6-point-per-decade approach.

3.4 DATA ACQUISITION

It involved establishing equipment at key locations of interest, after which electrodes were placed. The resistance values were measured and documented using an ABEM Tetrameter 300 machine. The Schlumberger electrode array was utilized, and the spacing for the electrodes followed a six-point-per-decade system

3.5 FIELD PRECAUTIONS

The following were adhered to in order to avoid errors during the acquisition of data:

Good contact was ensured between the reel wires and the electrodes.

The electrodes were properly hammered down to ensure good contact with the ground.

Avoidance of power lines was paramount to avoid distortion of resistance readings

Disconnecting of the reels from the tetrameter while reels were rotating was ensured to avoid tangling.

Avoidance of crossing of potential and current reel wires was ensured to avoid tangling.

3.6 ADJUSTED DATA

This section presents the outcome of the data reduction process, which entails plotting the apparent resistivity values on the vertical axis against the current electrode spacing (AB/2) on a log-log graph, either manually or with electronic tools. Following this step, the curve is examined for its smoothness, and modifications can subsequently be made to improve the curve's smoothness. Adjusting these values to create a more consistent curve leads to the adjusted values.

3.7 INTERPRETATION TECHNIQUE

In this section, the Quantitative interpretation technique is utilized. The measured apparent resistivity values are plotted against the current electrode position AB/2 (m), with A and B representing the two current electrode locations, on double logarithmic paper of standard size 62.5mm per decade. When employing this method, focus is given to the shape of the field curve, particularly concerning the relationship between neighboring branches in cases with three layers. Four typical relationships or curves, labeled H, K, A, and Q, correspond to Bowl type, Bell type, ascending type, and descending type curves, respectively, identified for the apparent resistivity field curves. Identifying the number of layers and their thicknesses within the curve is referred to as quantitative interpretation. Geo-electric parameters were manually extracted from the adjusted resistivity values after they were smoothed using Microsoft Excel software. IX1D and Surfer software were employed for the final stages of interpretation, which included analyzing lithology, determining depth to groundwater, and generating a Geo-electric section illustrating the lithologies.

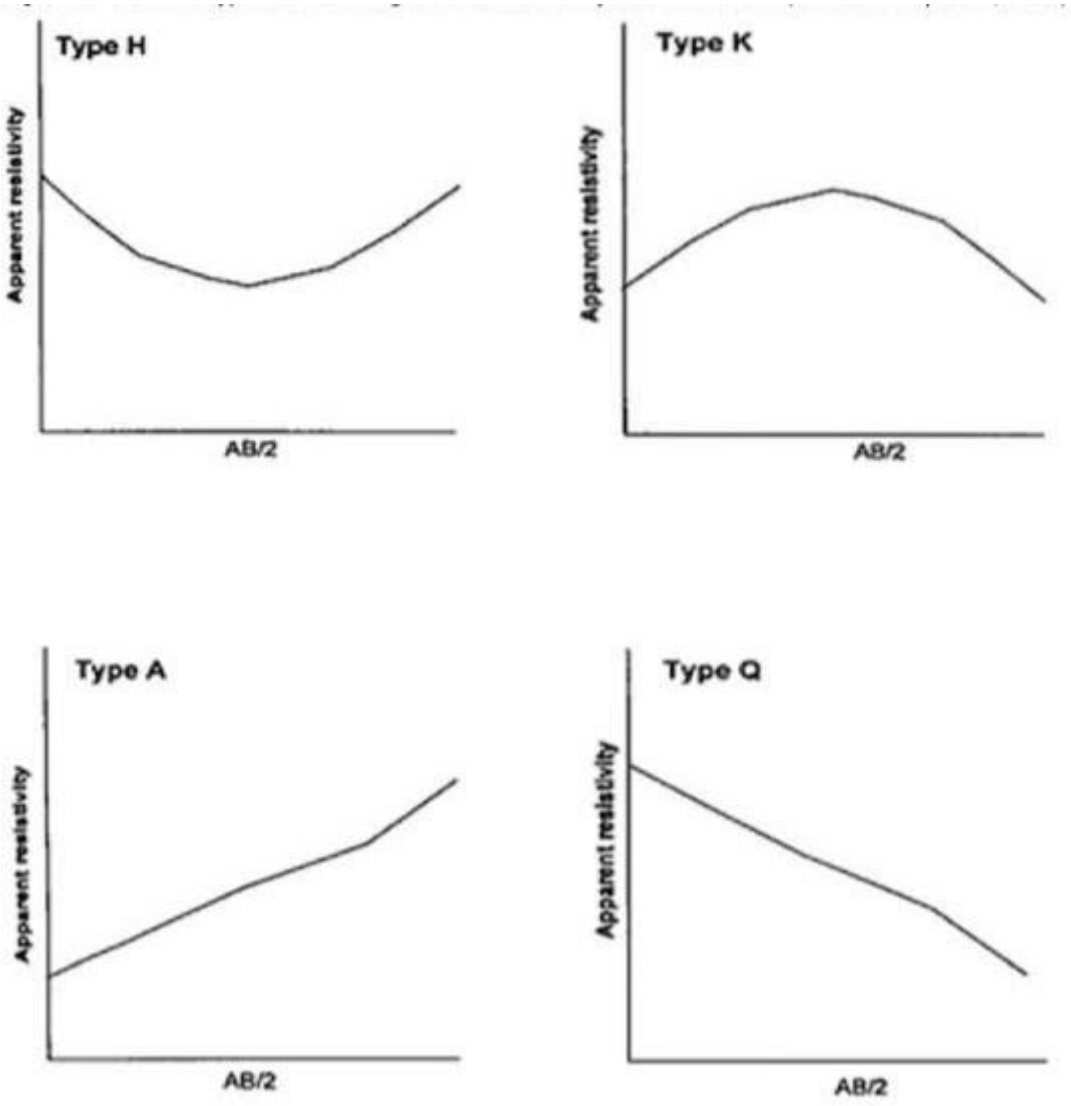

Fig 3.2: Diagram of resistivity curves (after Gopinath & Seralathan, 2003)

CHAPTER FOUR

RESULTS AND DISCUSSION

4.1 RESULTS

The study results are presented in the form of Geo-Electric sections, that represents the resistivity curves and tables. Figures 4.1 – 4.4 display the results of the four VES curves (Vertical Electrical Sounding) which were obtained from the adjusted values of apparent resistivity acquired from the field.

VERTICAL ELECTRICAL SOUNDING [VES] SCHLUMBERGER ARRAY FIELD RECORD

COORDINATES: N: 6° 22′ 48″ E: 5° 35′ 60″

SOUNDING NUMBER: VES: JJV1

TABLE 1: Results for VES JJV1

COORDINATES: N: 6° 22′ 43.79″ E: 5° 35′ 0.43″

SOUNDING NUMBER: VES: JJV2

TABLE 2: Results for VES JJV2

AB/2 (m)	MN/2 (m)	ADJUSTED RESISTIVITY
1.00	0.2	103.15
1.47	0.2	94.89
2.15	0.2	98.26
3.16	0.2	109.34
4.64	0.2	125.09
6.81	0.2	169.88
10	2.0	188.75
14.7	2.0	265.53
21.5	2.0	347.40
36.1	2.0	409.81
46.4	10	502.64
68.1	10	556.38
100	10	651.95
147	40	713.82
190	40	690.71

AB/2 (m)	MN/2 (m)	ADJUSTED RESISTIVITY

1.00	0.2	72.140
1.47	0.2	85.290
2.15	0.2	110.16
3.16	0.2	131.59
4.64	0.2	164.09
6.81	0.2	198.74
10	2.0	231.47
14.7	2.0	290.53
21.5	2.0	356.41
31.6	2.0	482.08
46.4	10	600.21
68.1	10	792.42
100	10	1072.9
147	40	1351.7
190	40	1585.0

COORDINATES: N: 6° 22′ 48″ E: 5° 22′ 50″

SOUNDING NUMBER: VES: JJV3

TABLE 3: Results for VES JJV3

AB/2 (m)	MN/2 (m)	ADJUSTED RESISTIVITY
1.00	0.2	343.82
1.47	0.2	283.26
2.15	0.2	244.96
3.16	0.2	244.34
4.64	0.2	261.68
6.81	0.2	327.24
10	2.0	400.69
14.7	2.0	461.85
21.5	2.0	540.00
31.6	2.0	593.56
46.4	10	675.20
68.1	10	713.00
100	10	730.85
147	40	702.70
215	40	601.46

COORDINATES N: 6° 22′ 52″ E: 5° 22′ 55″

SOUNDING NUMBER: VES: JJV4

TABLE 4: Results for VES JJV4

AB/2 (m)	MN/2 (m)	ADJUSTED RESISTIVITY
1.00		
1.47		
2.15		
3.16		
4.64		
6.81		
10		
14.7		
21.5		
31.6		
46.4		
68.1		
100		
147	40	1120.3
215	40	1205.8
316	40	1185.3

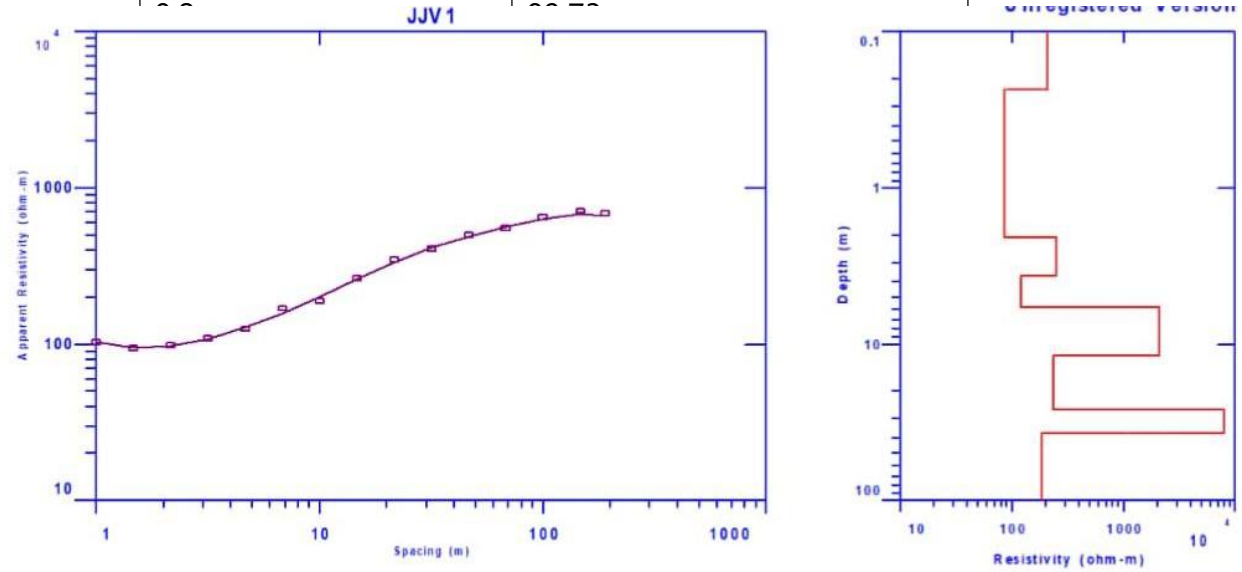

Fig 4.1 : VES 1 interpretation results. Left: Resistivity Curve; Right: Interpreted Geo model.

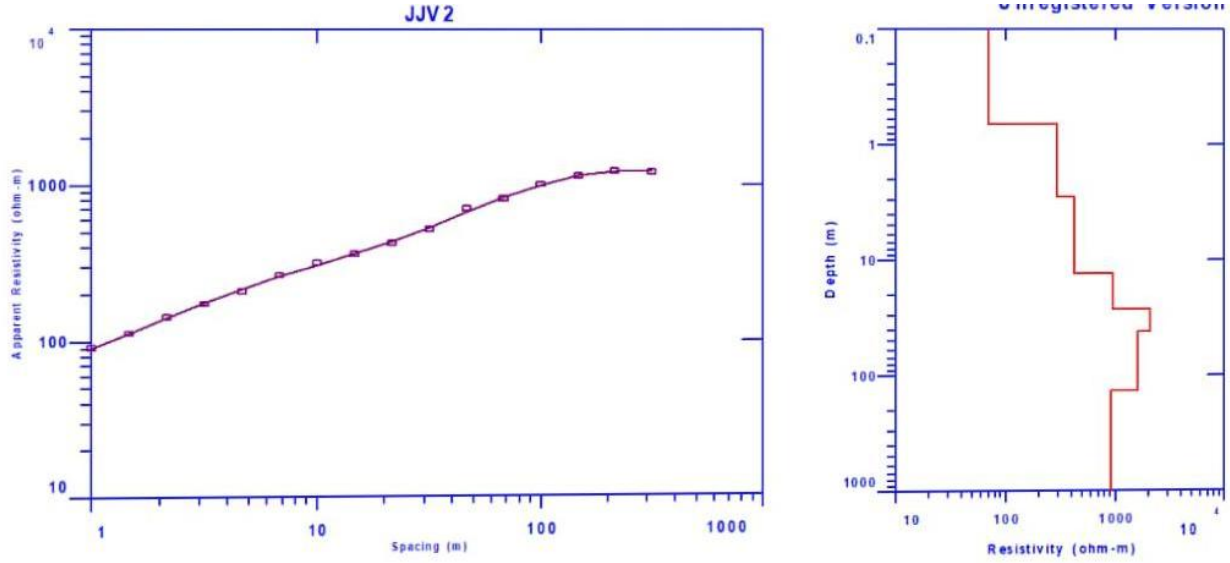

Fig 4.2: VES 2 interpretation results. Left: Resistivity Curve; Right: Interpreted Geo model.

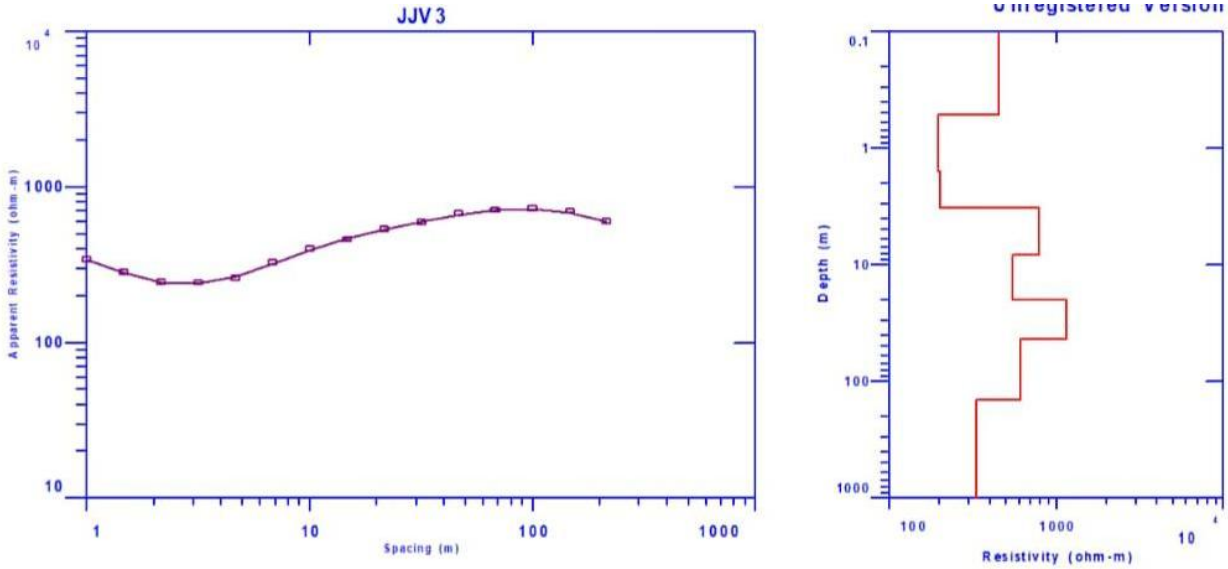

Fig 4.3: VES 3 interpretation results. Left: Resistivity Curve; Right: Interpreted Geo model.

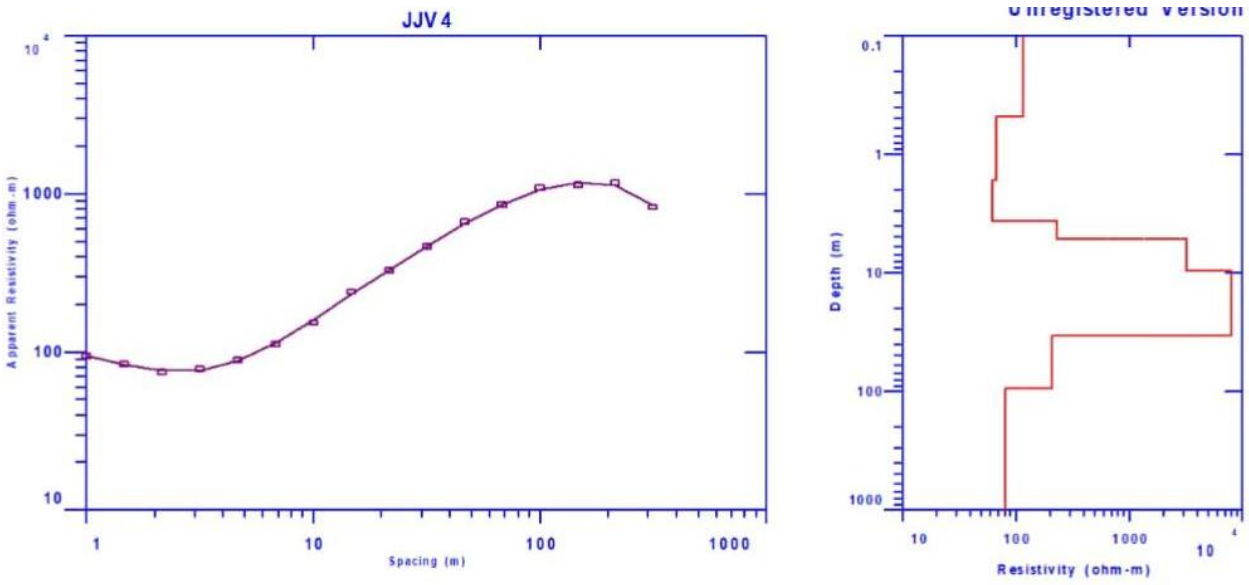

Fig 4.4: VES 4 interpretation results. Left: Resistivity Curve; Right: Interpreted Geo model.

THE INTERPRETED VES RESULTS AND THE CORRESPONDING INFERRED LITHOLOGY

TABLE 5: Geological model of VES JJV1

Geo-Electric Layers	Resistivity of Layers (m)	Thickness (m)	Depth (m)	Inferred Lithology
1	206.84	0.23401	0.23401	Topsoil
2	84.859	1.8354	2.0694	Clay
3	247.66	1.5962	3.6656	Sand
4	121.89	2.1263	5.7919	Clayey sand
5	2084.0	5.9539	11.746	Sand (dry)
6	235.26	14.326	26.072	Lateritic sand
7	7977.5	11.194	37.266	Dry sand
8	183.20			Sand (saturated)

TABLE 6: Geological model of VES JJV2

Geo-Electric Layers	Resistivity of Layers (m)	Thickness (m)	Depth (m)	Inferred Lithology
1	451.61	0.51547	0.51547	Topsoil
2	195.72	1.0673	1.5828	Clayey sand
3	202.12	1.6465	3.2293	Lateritic sand
4	793.56	5.0621	8.2913	sand
5	544.57	11.620	19.911	Lateritic sand
6	1144.0	23.159	43.070	Dry sand
7	606.83	99.629	142.70	Sand (saturated)
8	333.83			Sand (saturated)

TABLE 7: Geological model of VES JJV3

Geo-Electric layers	Resistivity of Layers (m)	Thickness (m)	Depth (m)	Inferred Lithology
1	71.041	0.68507	0.68507	Topsoil
2	290.52	2.0332	2.7183	Laterite sand
3	424.68	11.322	14.040	Laterite sand

4	1013.8	13.485	27.525	Sand
5	2575.2	14.038	41.563	Sand (dry)
6	1783.4	13.393	54.556	Sand (saturated)
7	1168.8			Sand (saturated)

TABLE 8: Geological model of VES JJV4

TABLE 9: Hydrogeological representation of the VES Data

Geo-Electric Layers	Resistivity of Layers (m)	Thickness (m)	Depth(m)	Inferred Lithology
1	116.53	0.48102	0.48102	Topsoil
2	66.546	1.1659	1.6469	Clay
3	62.370	1.9807	3.6276	Clay
4	231.46	1.5496	5.1772	Lateritic sand
5	3169.9	4.4730	9.6502	sand
6	7963.0	24.134	33.784	Dry sand (dry)
7	207.94	59.439	93.222	Sand (saturated)
8	80.477			Sand (saturated)

LATITUDE	LONGITUDE	SURFACE ELEVATION (m)	DEPTH TO WATER TABLE (m)	ELEVATION OF WATER TABLE (m)	ISO RESISTIVITY	VES NUMBER
6° 22′ 48″	5° 35′ 60″	105	37.266	67.734	183.20	JJV1
6° 22′ 43.79″	5° 35′ 0.43″	103	60.326	42.674	606.83	JJV2
6° 22′ 48″	5° 22′ 50″	105	43.070	61.930	1783.4	JJV3
6° 22′ 52″	5° 22′ 55″	103	33.784	69.216	207.94	JJV4

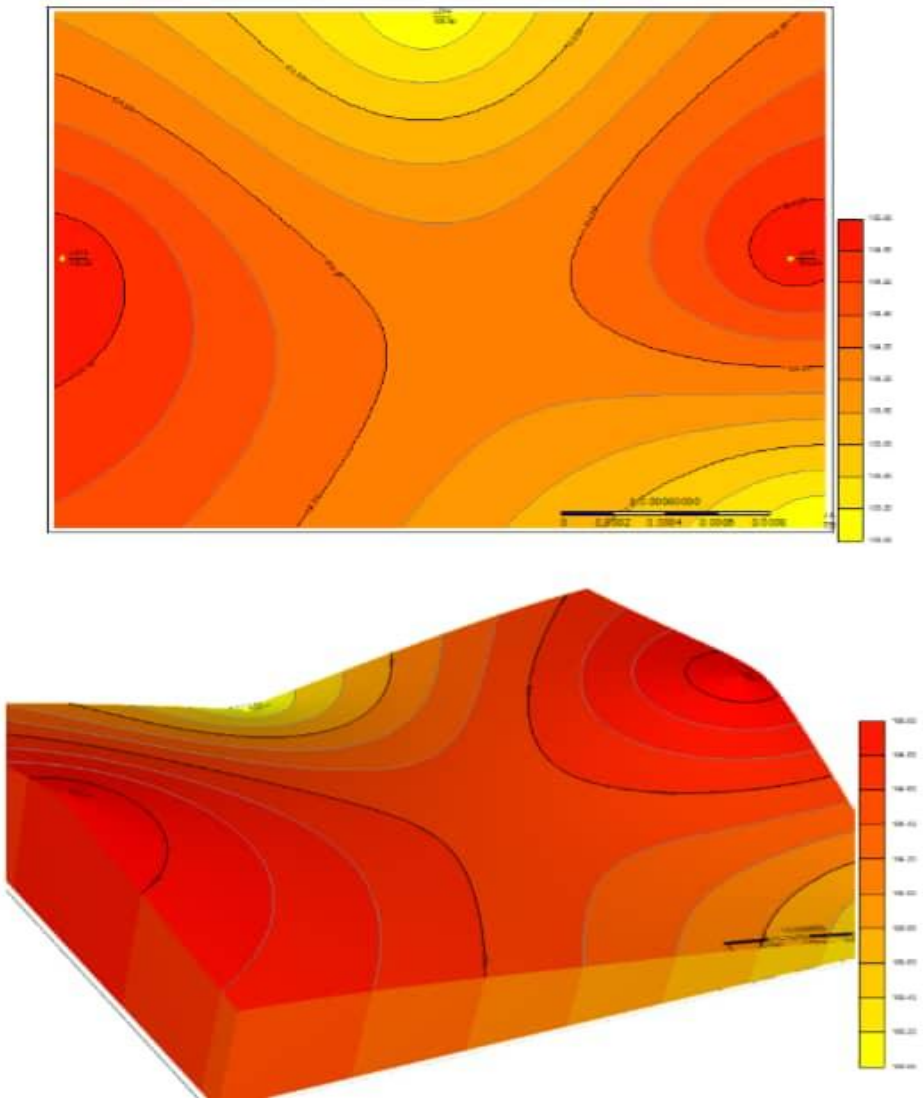

Fig. 4.5: Map of Surface Elevation: Top: 2D Map; Bottom: 3D Map

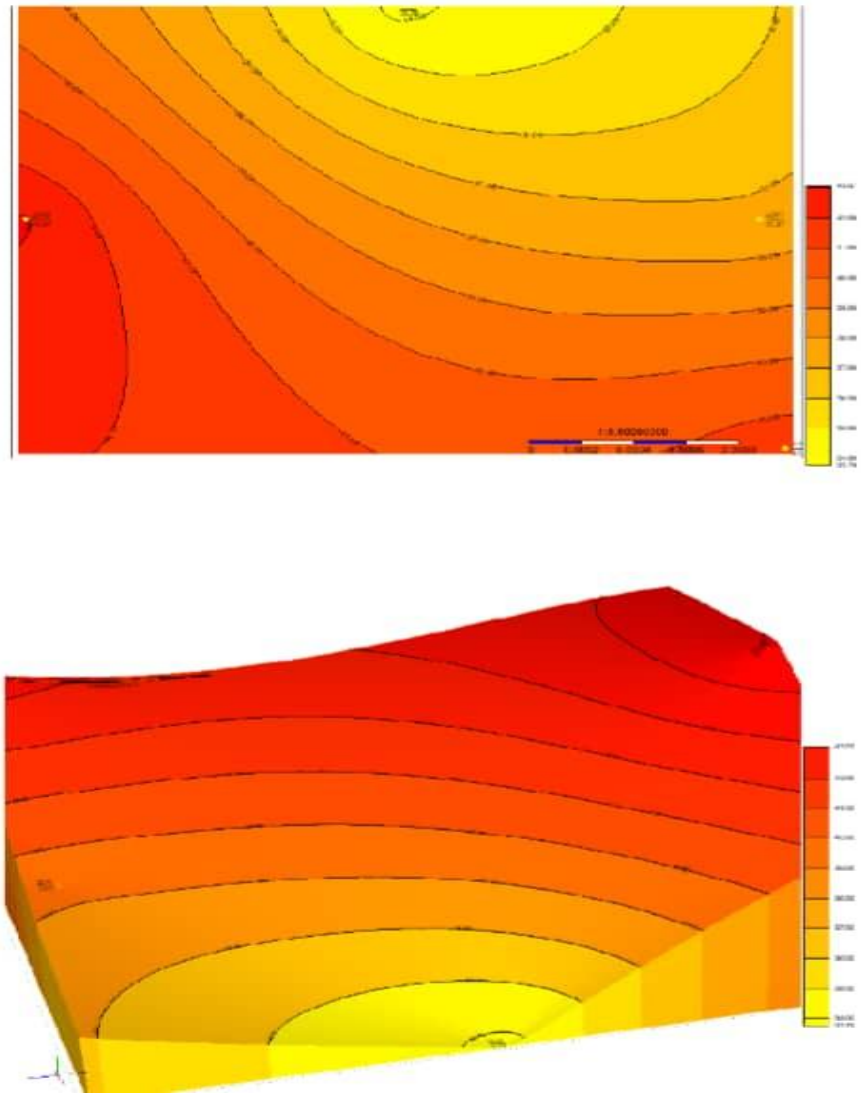

Fig. 4.6: Map of depth to Depth to water table: Top: 2D Map; Bottom: 3D Map

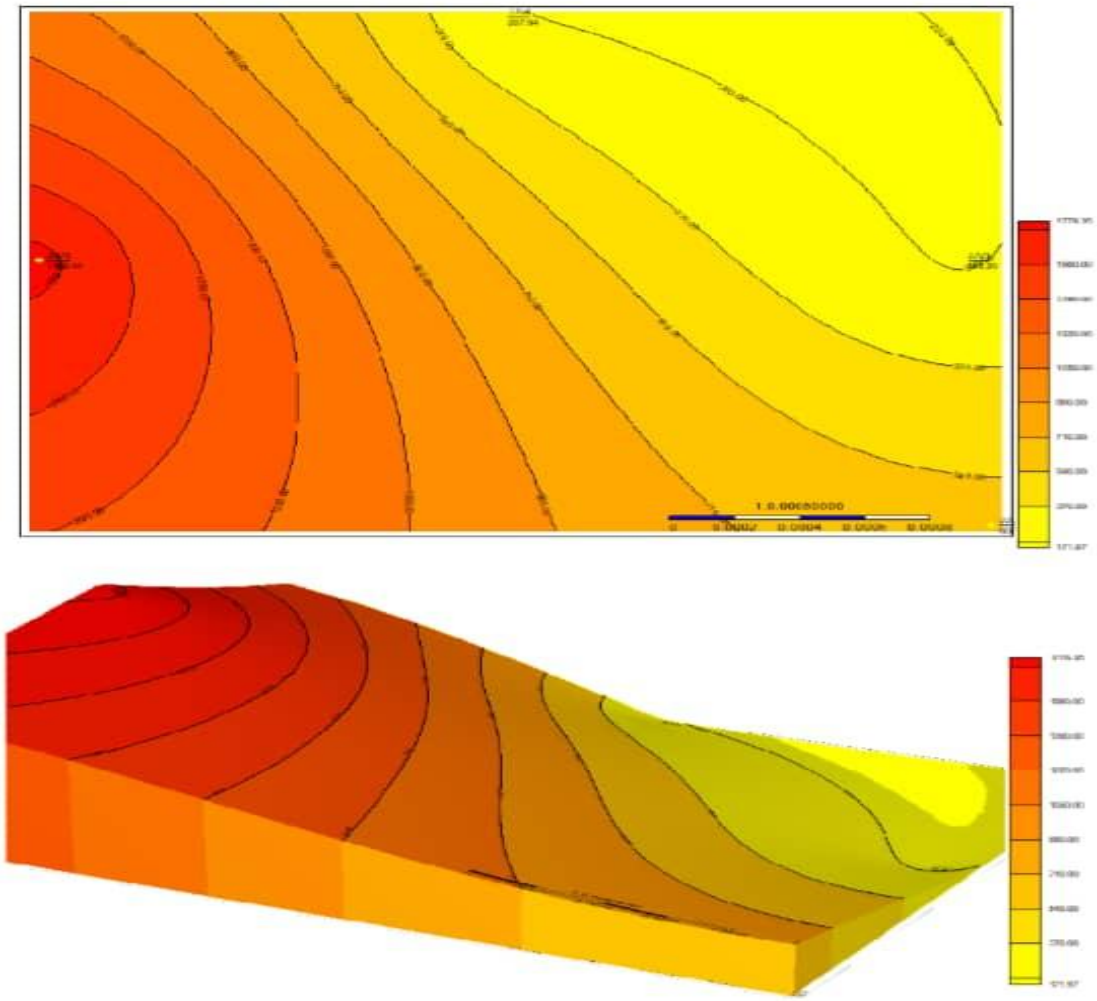

Fig. 4.7: Equi-potential map: Top: 2D Map; Bottom: 3D Map

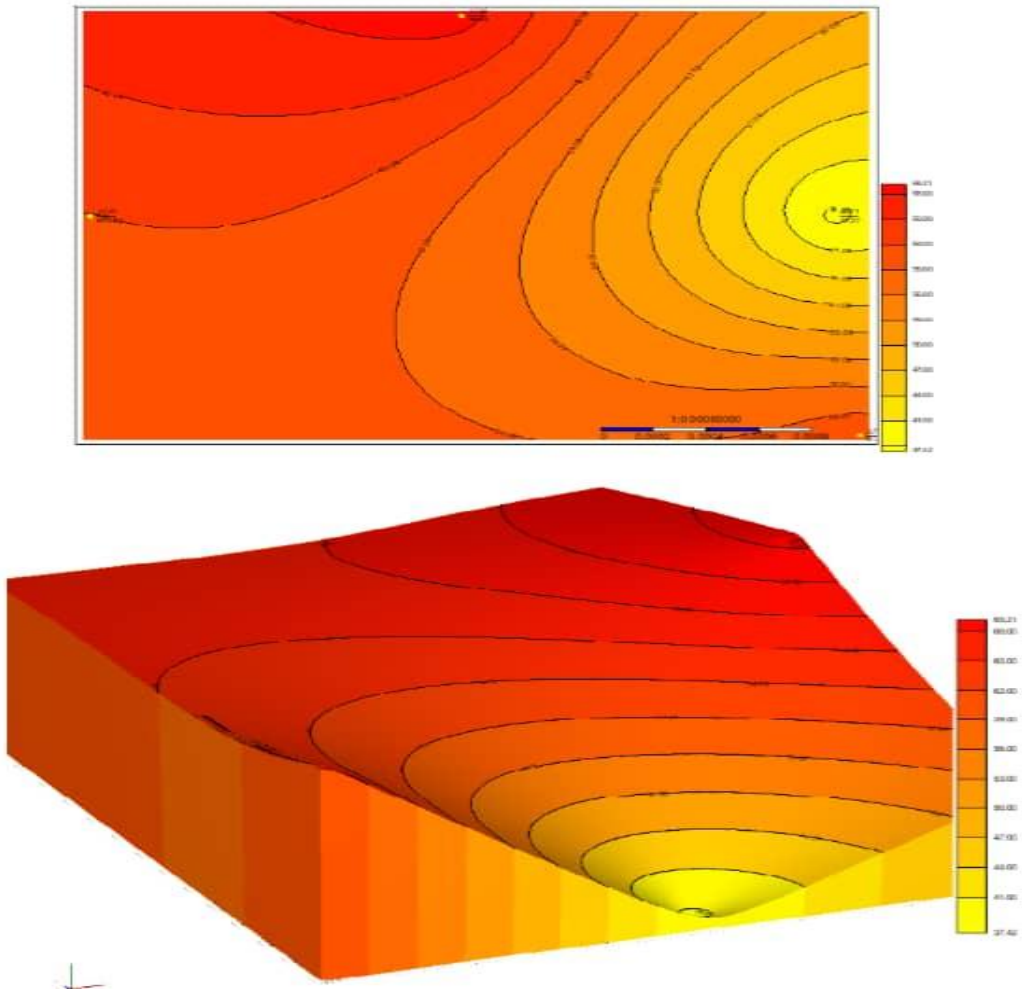

Fig. 4.8: Map of Iso-resistivity: Top: 2D Map; Bottom: 3D Map

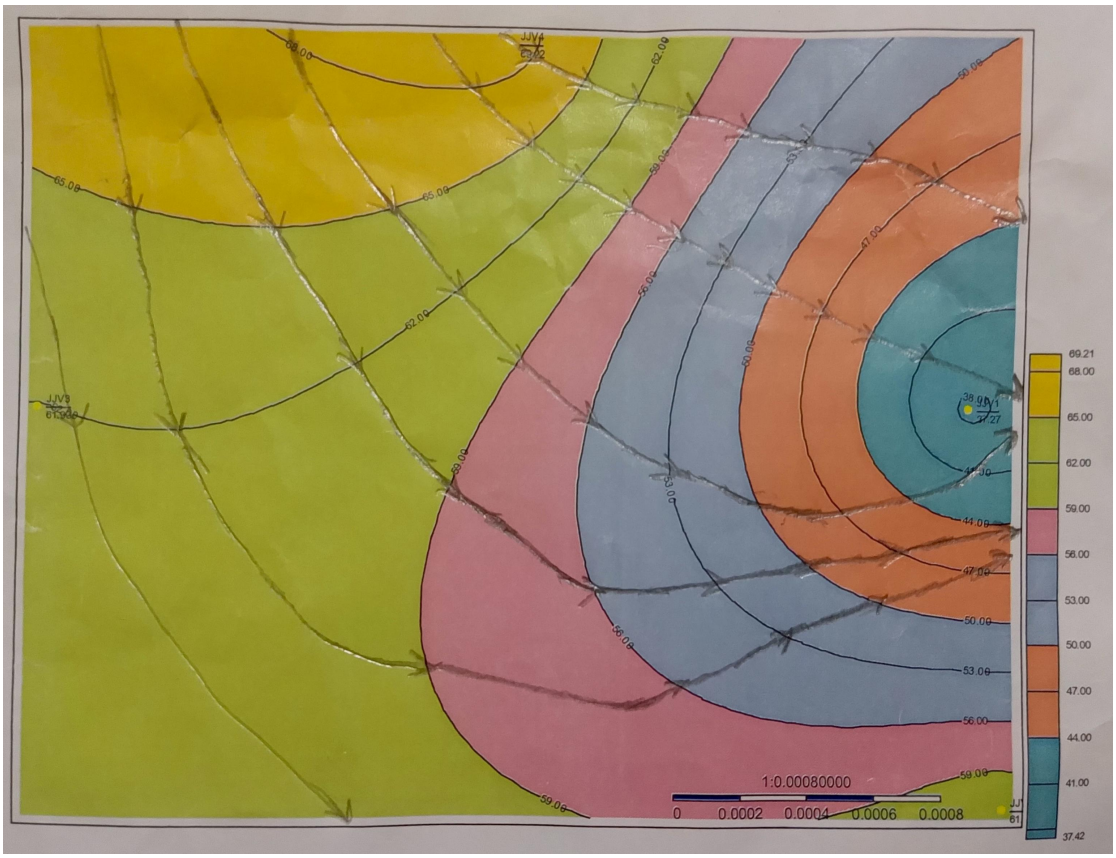

Fig 4.9: Local ground water flow map

DISCUSSION

Based on the surface elevation data of the map in Fig 4.5, it is observed that the elevation at VES locations JJV1 and JJV3 is 105 meters, while at JJV2 and JJV4, the elevation is slightly lower at 103 meters. This indicates a minor variation in surface elevation across the study area, with a slight depression observed at JJV2 and JJV4. Given that surface elevation can influence groundwater flow and vulnerability, these minor differences may indicate localized variations in surface runoff and infiltration. However, the relatively close elevation values suggest a generally consistent surface condition across the VES points. This data provides a baseline for understanding the relationship between surface topography and subsurface groundwater conditions as interpreted from the VES results.

From the ‘depth to water table‘ data of Fig 4.6, it can be observed that the water table is shallowest at VES location JJV4, with a depth of 33.784 meters. Conversely, the water table is deepest at VES location JJV2, with a depth of 60.326 meters. The water table depths at JJV1 and JJV3 are intermediate, at 37.266 meters and 43.070 meters respectively. This variation indicates a significant difference in groundwater depth across the study area. The shallower water table at JJV4 suggests a higher susceptibility to contamination from surface activities, while the deeper water table at JJV2 provides a greater buffer against such contamination due to the increased distance for contaminants to travel before reaching the groundwater. These depth variations should be considered when planning borehole development to ensure both adequate water supply and protection from potential contamination.

By studying ’the elevation of the water table‘ data in Fig 4.7, it can be observed that the water table elevation is highest at VES location JJV4, with an elevation of 69.216 meters. Conversely, the water table elevation is lowest at VES location JJV2, with an elevation of 42.674 meters. The water table elevations at JJV1 and JJV3 are intermediate, at 67.734 meters and 61.930 meters respectively. This variation indicates a significant difference in groundwater elevation across the study area. The higher

water table elevation at JJV4 suggests a potential area of groundwater recharge or higher hydraulic head, while the lower water table elevation at JJV2 indicates a potential area of groundwater discharge or lower hydraulic head. These elevation variations should be considered when analyzing groundwater flow direction and potential aquifer productivity.

The observation made on the Iso-resistivity data, it can be examined that the resistivity values of 4.8 vary significantly across the study area. The lowest resistivity value is 183.20 Ohm-m, while the highest is 1783.4 Ohm-m. Intermediate values are 606.83 Ohm-m and 207.94 Ohm-m. This variation in resistivity indicates differences in subsurface lithology and groundwater presence. Lower resistivity values generally suggest the presence of conductive materials, such as saturated sands or clays, while higher resistivity values indicate resistive materials, such as dry sands or lateritic formations. These variations should be considered when interpreting the groundwater potential and planning borehole development in the study area.

Based on the map of Fig 4.9, the local groundwater flow is inferred to follow the surface elevation, moving from higher to lower points. Specifically, the map suggests that water flows from the north-northwest towards the south-southeast region. This flow pattern indicates that the groundwater movement is influenced by the surface topography, with water likely recharging in the higher elevation areas and discharging in the lower elevation areas. The direction of flow also suggests that the subsurface geology and hydraulic conductivity in this region support this general movement of groundwater.

CONCLUSION

The geoelectric investigation conducted in Uwasota and environs, Benin City, Southern Nigeria, successfully delineated subsurface lithologies and assessed groundwater potential using Vertical Electrical Sounding (VES) with the Schlumberger array. The results are consistent with the established literature on the Benin Formation, which comprises predominantly sands with minor clay content, varying in grain size. Resistivity analysis revealed distinct lithological units: topsoil (71.041Ωm-451.61Ωm), dry sand (1144.0Ωm-7977.5Ωm), clay (62.370Ωm-84.859Ωm), lateritic sand (202.12Ωm-544.57Ωm), clayey sand(121.89Ωm-195.72Ωm) and a saturated sand aquifer (80.477Ωm-1783.4Ωm).

The identified saturated sand aquifer, found at depths ranging from 73.4m to 134.2m below ground surface, confirms the area's potential as a viable source of potable water. This aligns with the Benin Formation's reputation as one of Nigeria's most prolific aquifers. The aquifer's depth and yield suggest it can support both residential and industrial water supply needs.

This study provides valuable insights for groundwater resource management in the region. To further enhance understanding and facilitate sustainable development, it is recommended that additional VES studies be conducted in the surrounding areas. These studies should aim to develop a groundwater flow map, enabling informed borehole placement for community water needs.

.

REFERENCES

Alabi, A. A., Daniel, E. E., & Udoh, F. D. (2010). Evaluating the geoelectric and hydraulic characteristics of some aquifers in parts of the Chad Formation, Northeastern Nigeria. Journal of Geology and Mining Research, 2(6), 136-143.

Afuwai, J. A. (2013). Geophysical Investigation of Groundwater Potential in Parts of Gombe Metropolis, Northeastern Nigeria. Journal of Earth Sciences and Geotechnical Engineering, 3(2), 1-14.

Alisiobi, A. O., & Ako, B. D. (2012). Assessment of groundwater potential in parts of Gombe and environs, northeastern Nigeria, using remote sensing and geophysical techniques. International Journal of Water Resources and Environmental Engineering, 4(10), 330-341.

Andrews, R.J., Barker, R. and Loke, M.H. (1995). The application of electrical tomography in the study of the unsatured zone in chalk at three sites in Cambridgeshire, United Kingdom. Hydrogeo. J. 3, 17-31.

Ariyo, S. O. (2005). Assessment of groundwater quality in a landfill environment, Ibadan, Nigeria. Journal of Environmental Hydrology, 13, 1-10.

Banton, O., Seguin, M.K. and Cimon, M.A. (1997). Mapping field scale physical properties of Soil with Electrical resistivity. Soil Sci. Soc. Am. J. 61, 1010-1017.

Bertrand, Y. (1967). Electrical prospecting applied to problems of Bridges and Roads. Bulletin Liaison des Laboratoires Routiers Paris -XV.

Burger, H. R., Sheehan, A. F., & Jones, C. H. (2006). Introduction to applied geophysics: exploring the shallow subsurface. WW Norton & Company.

Danielsen, M., Midtgård, H., & Ramstad, K. (2007). Geoelectrical investigations of saline groundwater intrusion in coastal aquifers. Journal of Applied Geophysics, 62(3), 195-207.

Doust, H., & Omatsola, E. (1989). Niger delta. AAPG Special Volumes 132,201-238

Gopinath, G. and Seralathan, P. (2003). Evaluation of Aquifer Parameters of the Muvattupha River Basin, Kerala.

Hasan (2017). Schlumberger Array: Electrical Resistivity Methods, Part 2

Helaly, A. (2017). Application of Vertical Electrical Sounding (VES) Technique for Groundwater Exploration in El-Farafra Oasis, Western Desert, Egypt. NRIAG Journal of Astronomy and Geophysics, 6(1), 164-175.

Kearey, P., Brooks, M., and Hill, I. (2002). An Introduction to Geophysical Exploration. 3rd Edition, Blackwell Science Ltd., Oxford. 262 Pgs, ISBN 0-632-04929-4.

Lile, O.B., Backe, H.R., Elvebakk, H. and Buan, J.E. (1994). Resistivity measurements on the sea bottom to map fractures zones in the bedrock underneath sediments. Geophy. Prospec. 42, 813-824.

Nowroozi, A. A., Horrocks, R. D., & Henderson, C. L. (1999). Delineation of subsurface freshwater zones in a coastal area using the geoelectrical method. Journal of Hydrology, 223(1-2), 49-65.

Michael, G., Ibukun, O., & Daniel, I. O. (2022). Geo-electrical investigation of ground water potential using vertical electrical sounding. World Journal of Advanced Research and Reviews, 15(2), 322-329.

Meheni, Y., Guérin, R., Benderitter, Y. and Tabbagh, A. (1996). Subsurface DC resistivity mapping: approximate 1-D interpretation. J. Appl. Geophy. 34, 255-270.

OEPA (Ondo State Environmental Protection Agency). (2008). State of the Environment Report. Akure, Nigeria: Ondo State Environmental Protection Agency.

Olayinka, A. I. (1992). Geoelectric sounding for groundwater in crystalline basement areas: a case study from Ile-Ife area, Nigeria. Journal of African Earth Sciences (and the Middle East), 15(4), 441-449.

Oluwajana, O. A., Ehinola, O. A., Okeugo, C. G., & Adegoke, O. (2017). Modeling hydrocarbon generation potentials of eocene source rocks in the agbada formation, Northern Delta Depobelt, Niger delta Basin, Nigeria. Journal of Petroleum Exploration and Production Technology, 7, 379-388.

Oseji, J. O., Ofomola, M. O., & Oborie, E. (2006). Geoelectric survey for groundwater in parts of Warri metropolis, Nigeria. Journal of Applied Sciences and Environmental Management, 10(3), 119-123.

Owoyemi, A. O. D. (2005). Sequence stratigraphy of Niger Delta, Delta field, offshore Nigeria (Doctoral dissertation, Texas A & M University).

Ritz, M., Robain, H., Pervago, E., Albouy, Y., Camerlynck, C., Descloitres, M. and Mariko, A. (1999). Improvement to resistivity pseudosection modelling by removal of near-surface inhomogeneity effects: application to a soil system in south Cameroon. Geophy. Prospec. 47, 85-101.

Rui, L. & Walker, J. & Fitzpatrick, R. & Changming, L. (2023). Regional Water and Soil Assessment for Managing Sustainable Agriculture in China and Australia.

Short, K. C., & Stäuble, A. J. (1967). Outline of geology of Niger Delta. AAPG bulletin, 51(5), 761-779.

Stewart, M. T. (1982). Evaluation of electromagnetic methods for rapid mapping of salt-water interfaces in coastal aquifers. Ground Water, 20(5), 528-535.

USEPA (United States Environmental Protection Agency). (2000). Ground water and wellhead protection. EPA/625/R-00/007. Washington, DC: United States Environmental Protection Agency.

Telford, W.M., Geldart, L.P., and Sheriff, R.E. (1990). Applied Geophysics. 2nd Edition, Cambridge, Cambridge University press, 770 Pgs.

Walker, K. (2022). "Ancient systems keep water flowing". Nature Middle East. Nature.